

Weakening of the π^* - π^* dimerisation in 1,2,3,5-dithiadiazolyl radicals

C.P. Constantinides,^a D.J. Eisler,^a A. Alberola,^a E. Carter,^b D. Murphy^b and J.M. Rawson^{a,c*}

Weakening of the π^* - π^* dimerisation in 1,2,3,5-dithiadiazolyl radicals: Structural, EPR, magnetic and computational studies of dichlorophenyl dithiadiazolyls, Cl₂C₆H₃CN₂SSN[•]

Christos P. Constantinides,^a Dana Eisler,^a Antonio Alberola,^a Emma Carter,^b Damien Murphy^b and
Jeremy M. Rawson^{a,c*}

^a The Department of Chemistry, The University of Cambridge, Lensfield Road, Cambridge, UK CB2 1EW.

^b The School of Chemistry, Cardiff University, Main Building, Park Place, Cardiff, UK CF10 3AT

^c Department of Chemistry and Biochemistry, The University of Windsor, 401 Sunset Av., Windsor, ON, Canada N9B 3P4. E-mail: jmrawson@uwindsor.ca

Supporting Information

- Figure S1.** Temperature dependence of magnetic susceptibility (χ vs T and χT vs T) for radical **1**.
- Figure S2.** Temperature dependence of magnetic susceptibility (χ vs T and χT vs T) for radical **2**.
- Figure S3.** Temperature dependence of magnetic susceptibility (χ vs T and χT vs T) for radical **3**.
- Figure S4.** Temperature dependence of magnetic susceptibility (χ vs T and χT vs T) for radical **4**.
- Figure S5.** Temperature dependence of magnetic susceptibility (χ vs T and χT vs T) for radical **5**.
- Figure S6.** Temperature dependence of the reduced unit cell parameters for **2**; (left) temperature dependence of the cell parameters; (right) percentage change.
- Table T1.** Temperature dependence of the unit cell parameters of **2**.
- Figure S7.** Solid-State X-band VT-EPR for radical **3** recorded between 10-140 K.
- Figure S8.** Solid-State X-band VT-EPR for radical **3** recorded between 150-295 K showing the evolution of the $\Delta M_s = \pm 1$ transitions associated with the $S = 1$ state and the formally forbidden half-field $\Delta M_s = \pm 2$ transitions.
- Table T2.** Energies of the closed- (S) open-shell (S^*) singlet and triplet (T) states for the radical pair [HCN₂SSN[•]]₂ at intra-dimer S \cdots S distances of 2.90 – 3.60 Å.
- SUP-1** Discussion of crystallographic issues related to structure determinations of **1 – 5**.
- Figure S9.** Structure of **2** refined (a) without disorder in the reduced cell ($Z' = 1$); (b) with disorder in the reduced cell ($Z' = 1$); (c) in the super-cell ($Z' = 4$). Molecules in the asymmetric unit in colour (symmetry related molecules via translation along the crystallographic b -axis in grey)
- Figure S10.** View of reduced monoclinic ($C2/c$) setting (left) and super-cell ($P-1$) setting (right) of **5** viewed perpendicular to the stacking axis.
- Table T3.** Comparison of the ‘false’ high symmetry (grey background) and ‘true’ lower symmetry super-cell structures of **1 – 5**. The doubling of the crystallographic axes corresponding to the π -stacking direction are highlighted in red. N.B. Some discrepancies in unit cell parameters arise from different refinements when multiple data sets were measured.

Figure S1. Temperature dependence of magnetic susceptibility (χ vs T and χT vs T) for radical **1**. Dashed lines and solid lines represent fits to the extended Bleaney-Bowers model in the temperature region 5-200 K and 5-300 K respectively.

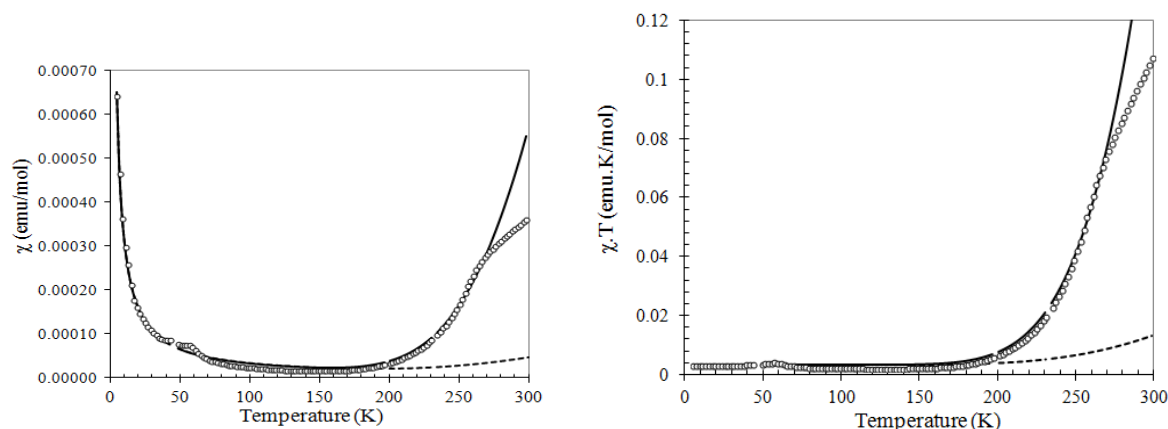


Figure S2. Temperature dependence of magnetic susceptibility (χ vs T and χT vs T) for radical **2**. Dashed lines and solid lines represent fits to the extended Bleaney-Bowers model in the temperature region 5-190 K and 5-300 K respectively.

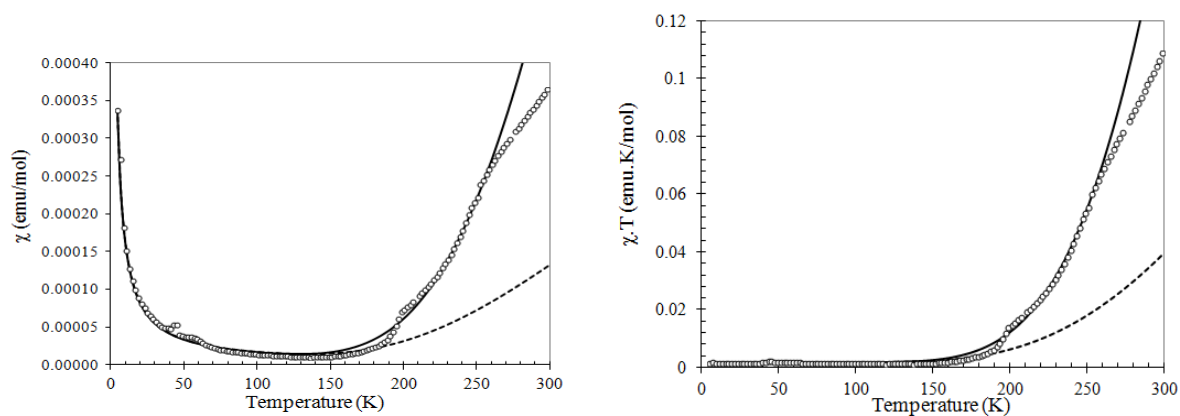


Figure S3. Temperature dependence of magnetic susceptibility (χ vs T and χT vs T) for radical **3**. Dashed lines and solid lines represent fits to the extended Bleaney-Bowers model in the temperature region 5-200 K and 5-300 K respectively.

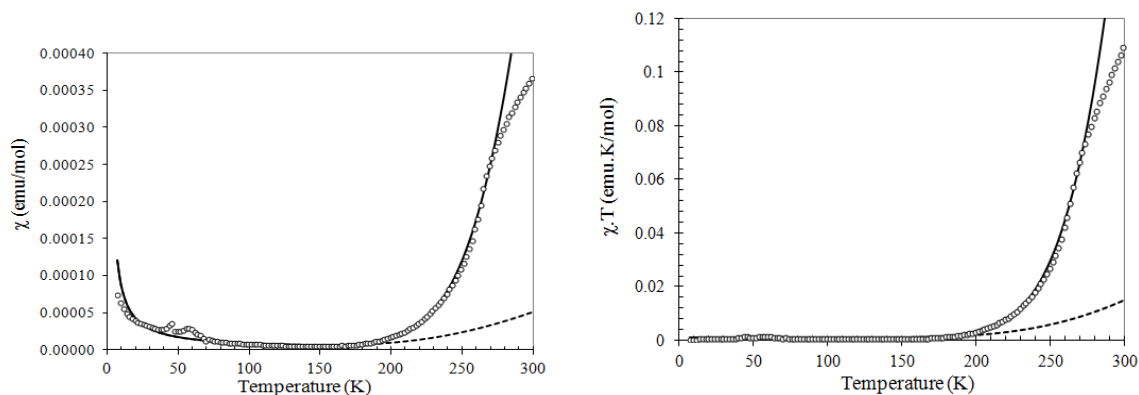


Figure S4. Temperature dependence of magnetic susceptibility (χ vs T and χT vs T) for radical 4. Dashed lines and solid lines represent fits to the extended Bleaney-Bowers model in the temperature region 5-240 K and 5-300 K respectively.

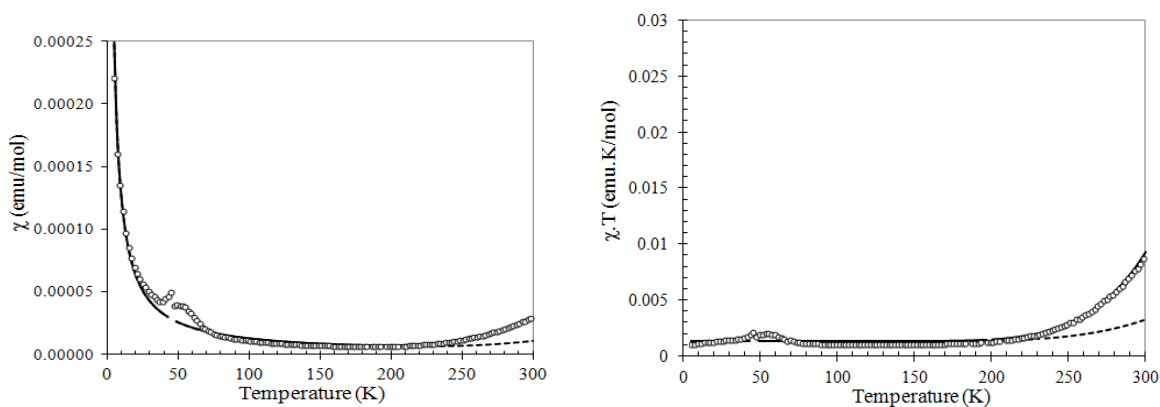


Figure S5. Temperature dependence of magnetic susceptibility (χ vs T and χT vs T) for radical 5. Dashed lines and solid lines represent fits to the extended Bleaney-Bowers model in the temperature region 5-200 K and 5-300 K respectively.

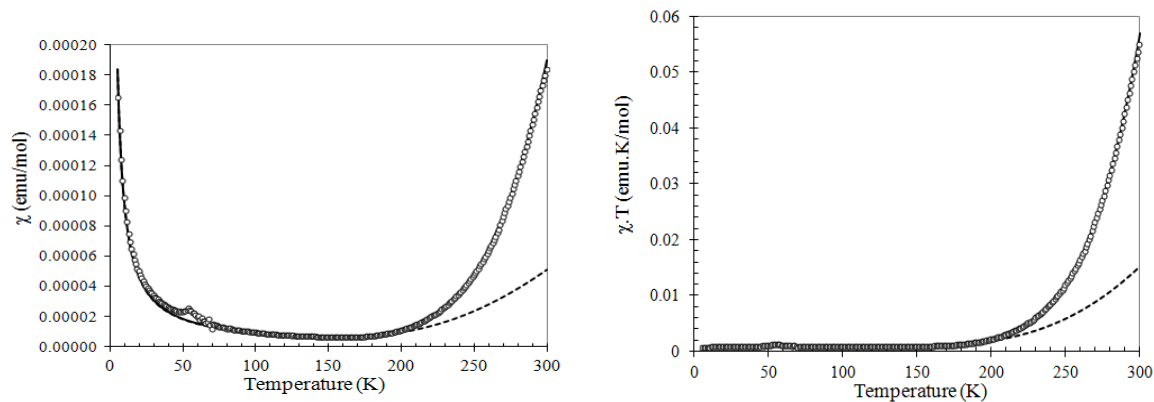
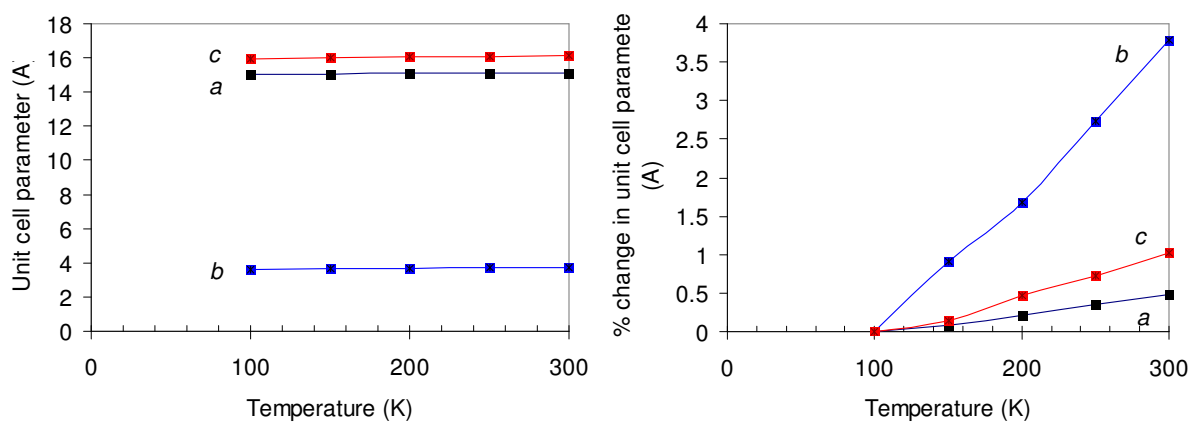


Figure S6. Temperature dependence of the reduced unit cell parameters for **2**; (left) temperature dependence of the cell parameters; (right) percentage change.**Table T1.** Temperature dependence of the unit cell parameters of **2**.

T/K	a	b	C	Δa	Δb	Δc	%change		
100	15.057	3.623	15.966	0	0	0	0	0	0
150	15.07	3.656	15.989	0.013	0.033	0.023	0.086339	0.910847	0.144056
200	15.089	3.684	16.04	0.032	0.061	0.074	0.212526	1.683688	0.463485
250	15.11	3.722	16.082	0.053	0.099	0.116	0.351996	2.732542	0.726544
300	15.13	3.76	16.13	0.073	0.137	0.164	0.484824	3.781397	1.027183

Figure S7. Solid-State X-band VT-EPR for radical **3** recorded between 10 and 140 K.

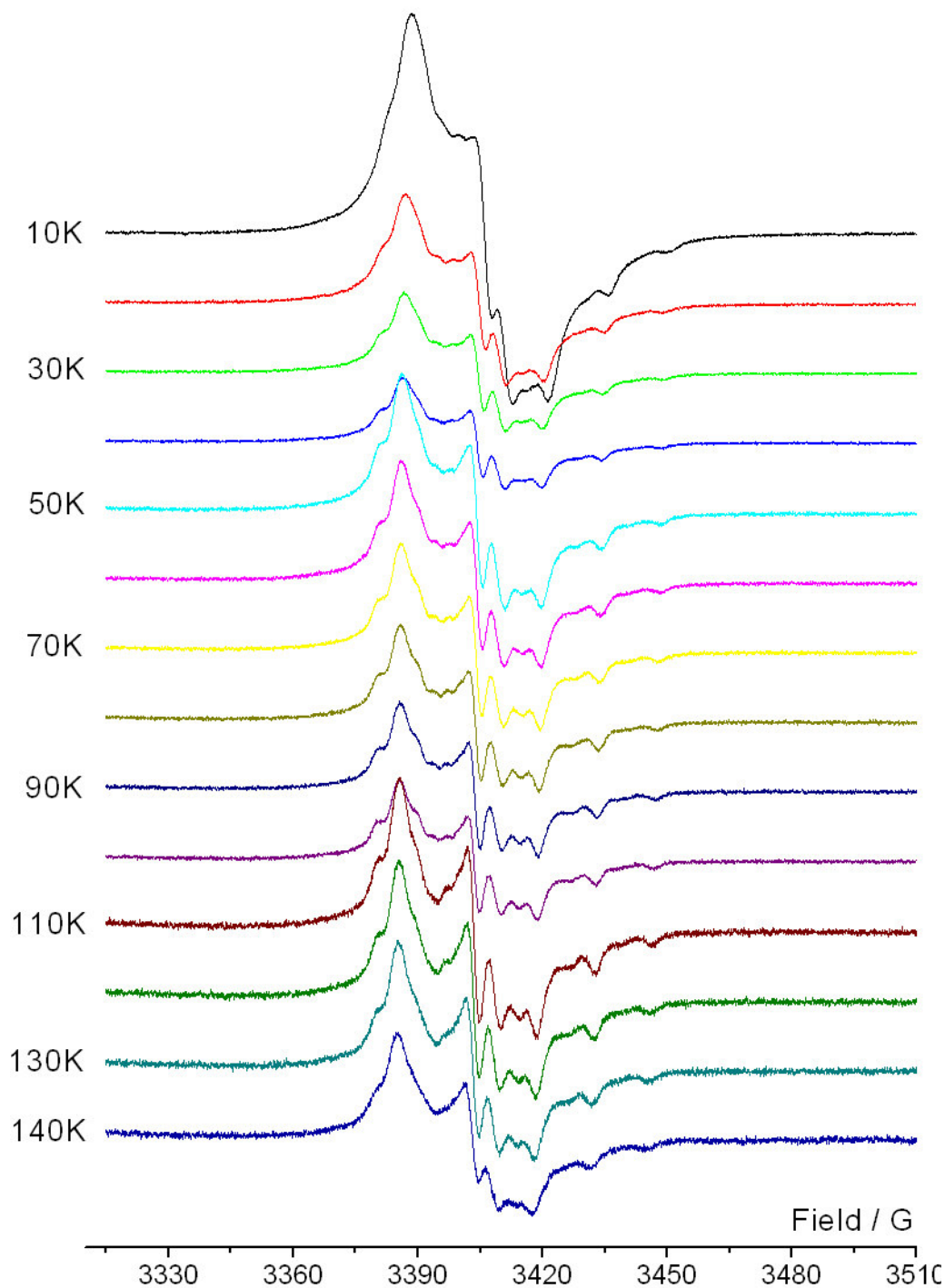


Figure S8. Solid-State X-band VT-EPR for radical **3** recorded in the range 150 - 295 K showing the evolution of the $\Delta M_s = \pm 1$ transitions associated with the $S = 1$ state and the formally forbidden half-field $\Delta M_s = \pm 2$ transitions.

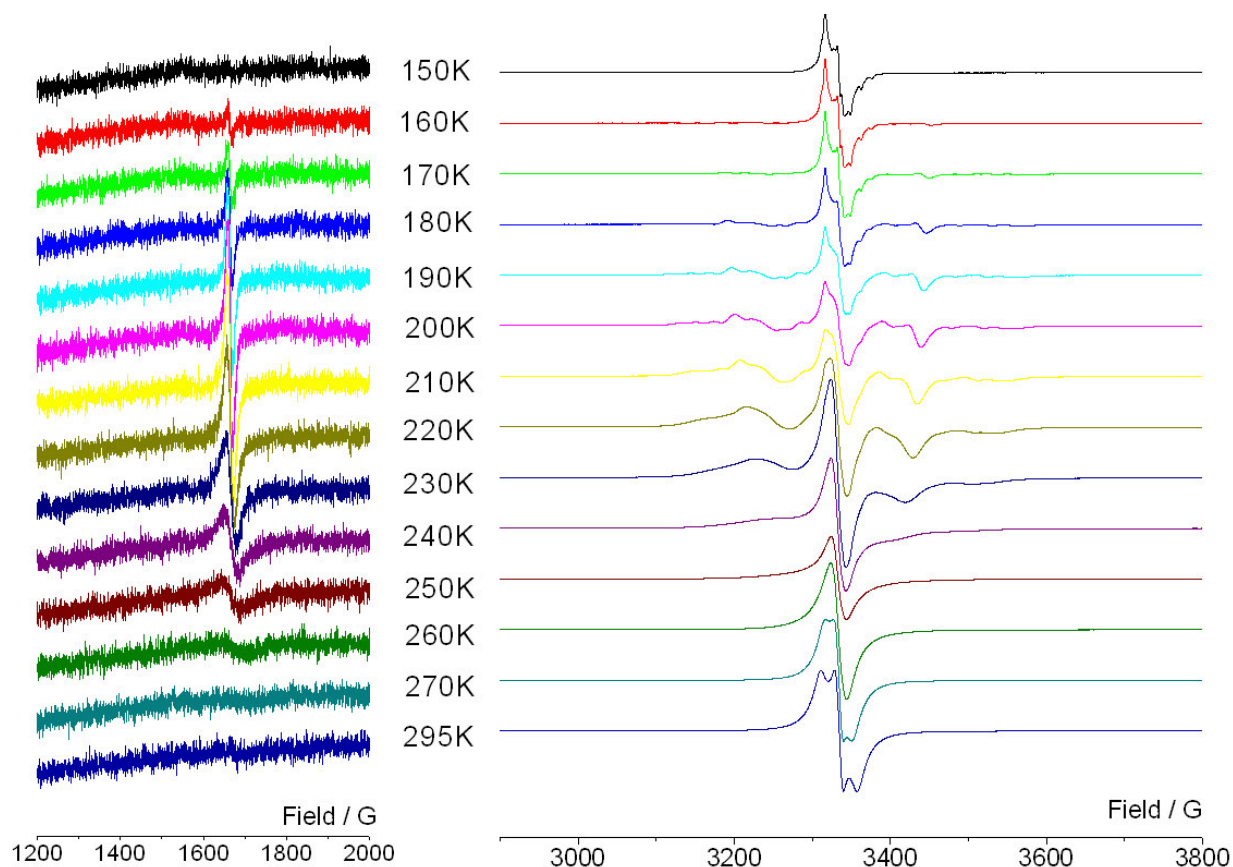


Table T2. Energies of the closed- (S) open-shell (S^*) singlet and triplet (T) states for the radical pair [HCN SSN]₂ at intra-dimer S \cdots S distances of 2.90 – 3.60 Å.¹

Intra-dimer S \cdots S distance (Å)	S (a.u.)	S^* (a.u.)	T (a.u.)
2.90	-1889.057888	-1889.057874	-1889.017393
3.00	-1889.062387	-1889.062363	-1889.031929
3.10	-1889.064526	-1889.064821	-1889.042773
3.20	-1889.065068	-1889.066835	-1889.050827
3.30	-1889.064503	-1889.068363	-1889.056768
3.40	-1889.063099	-1889.069484	-1889.061108
3.50	-1889.061460	-1889.070294	-1889.064253
3.60	-1889.059487	-1889.070868	-1889.066510

¹Calculations were performed using the B3LYP/6-31G* optimized geometry of the HCN $SSN\cdot$ while the energies of the three different states (S, S^* , T) were determined from single point calculations on the [HCN SSN]₂ radical pair at the UB3LYP/6-31G* level of theory.

SUP-1 Discussion of crystallographic issues related to structure determinations of **1** – 5.

The presence of π -stacked structures with near regular displacement of Cl atoms along the π -stacking direction led to persistent problems with identification of the correct cell and a persistent tendency for twinning in every structure. In every case cells with a short *ca.* 3.6 Å axis could be identified. Solutions in these small cells invariably revealed large displacement parameters for S and N parallel to the stacking axis, substantially larger than the U_{ij} for the Cl and C atoms of the aryl substituent, indicating the presence of disorder or a supercell. Such behaviour has been observed previously for 2,5-fluorophenyl dithiadiazolyl.¹ In many cases multiple datasets were collected over a range of temperatures from 100 K to 298 K in order to try and correctly identify the correct cell and space group. Whilst this was successful in some cases, the identification of an appropriate super-cell was a significant problem.

Structure of 1

An initial cell was identified [$a = 7.3579(15)$, $b = 13.615(3)$, $c = 17.984(4)$, $\alpha = 90$, $\beta = 101.78(3)$, $\gamma = 90^\circ$]. Whilst all non-hydrogen atoms were refined with anisotropic thermal displacement parameters. initial refinement stalled at 29.86% indicative of twinning, with many $F_{\text{obs}} > F_{\text{calc}}$ reflections. The application TwinRotMat within PLATON (Spek 2005) was used to determine the appropriate twin law and to generate an HKLF5 file for further refinement. The R values, K value, esds and background noise were all significantly improved, indicating the correct twin assignment [R_1 ($I > 2\sigma(I) = 4.32\%$)]. A test for higher symmetry using ADDSYM within PLATON detected a potential lattice centering or halving. The data were reprocessed with alternative C-centered cells ($a = 7.3579$, $b = 35.2177$, $c = 13.6134$ $\alpha = 90$ $\beta = 90.01$ $\gamma = 90^\circ$). However no suitable solution could be refined using this cell (for monoclinic or orthorhombic space groups) and the final structure retained the initial cell with $Z' = 2$ (one dimer) in the asymmetric unit.

Structure of 2

Initial indexing identified a monoclinic space group $P2_1/c$ with a short *b*-axis [$a = 15.074$, $b = 3.621$, $c = 16.098$, $\alpha = 90$, $\beta = 91.16$, $\gamma = 90^\circ$]. Structure solution afforded a single molecule in the asymmetric unit but with elongated ellipsoids for both heterocyclic S and N atoms. An examination of the disorder revealed a possible super-cell associated with a doubling of the crystallographic *b*-axis. No clear super-cell was evident from the observed data despite examining multiple crystals; a total of 3 data sets were collected over the range 100 - 273 K, prepared from 3 separate preparations in attempts to resolve this problem without success.

Eventually the original data were reprocessed in a larger super-cell [$a = 15.057(3)$, $b = 7.2462(14)$, $c = 15.986(3)$, $\alpha = 90$, $\beta = 91.32(3)$, $\gamma = 90^\circ$] corresponding to doubling of the short axis and the structure solved in *P-1* with four molecules in the asymmetric unit. Again refinement stalled with high residuals and a large number of $F_{\text{obs}} > F_{\text{calc}}$ were observed indicative of twinning. The application TwinRotMat within PLATON was used to determine the appropriate twin law, corresponding to reflection along the stacking axis, *b* [Twin Law 1 0 0 0 -1 0 0 0 1]. The inclusion of the Twin Law led to much improved residuals [R_1 ($I > 2\sigma(I) = 0.056$)] with $Z' = 4$ (two dimers per asymmetric unit), albeit with a low data:parameter ratio due to the

1 A.J. Banister, A. S. Batsanov, O.G. Dawe, P.L. Herbertson, J.A.K. Howard, S. Lynn, I. May, J.N.B. Smith, J.M. Rawson, T.E. Rogers, B.K. Tanner, G. Antorrena and F. Palacio, *Dalton. Trans.*, 1997, 2539; L. Beer, A.W. Cordes, D.J.T. Myles, R.T. Oakley and N.J. Taylor, *CrystEngComm.*, 2000, 2, 109.

C.P. Constantinides,^a D.J. Eisler,^a A. Alberola,^a E. Carter,^b D. Murphy^b and J.M. Rawson^{a,c*}

doubling of the b -axis. As a consequence of the poor statistics, all atoms were refined isotropically with a common U_{iso} for each element, leading to larger uncertainties in the geometric parameters. The structure of **2** in the monoclinic cell (i) as a regular π -stack without disorder; (ii) with disorder modeled over two sites and (iii) in the triclinic super-cell with discrete dimers are depicted in Fig. S.9.

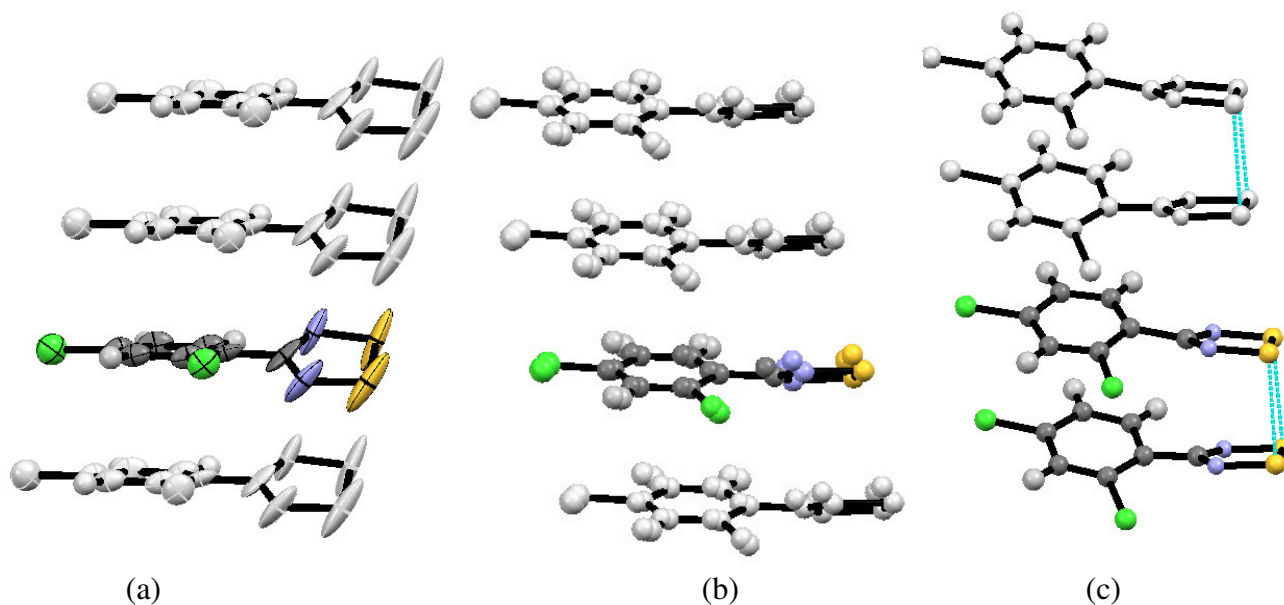


Figure S9. Structure of **2** refined (a) without disorder in the monoclinic $P2_1/c$ cell ($Z' = 1$); (b) with modelled disorder in the same cell ($Z' = 1$); (c) in the triclinic super-cell ($Z' = 4$). In the triclinic cell there are two crystallographically independent dimers; one is shown here. Molecules in the asymmetric unit are shown in colour (symmetry related molecules *via* translation along the crystallographic b -axis depicted in grey).

Structure of **3**

The structure of **3** has already been described.² However it, like **2**, initially offered a small monoclinic cell in the $P2_1/c$ setting [$a = 3.6506(7)$, $b = 24.358(5)$, $c = 10.170(2)$, $\beta = 97.54(3)^\circ$] with one molecule in the asymmetric unit. Whilst refinement proved satisfactory [R_1 ($I > 2\sigma(I)$) = 6.75%], the regular π -stack motif coupled with the elongated U_{ij} parameters for S and N atoms indicated the presence of a super-cell and the data were reprocessed in the triclinic $P-1$ setting [$a = 7.3271(2)$, $b = 10.3563(3)$, $c = 24.6666(7)$, $\alpha = 88.096(2)$, $\beta = 81.458(2)$, $\gamma = 77.0090(10)^\circ$] corresponding to a doubling of the a axis and a flipping of b and c . Once again, refinement in this lower symmetry setting stalled with high residuals and $F_{\text{obs}} > F_{\text{calc}}$ for many of the most disagreeable reflections indicating a twinned structure. In this instance the appropriate merohedral twin was determined using Rotax (S. Parsons and R. Gould, University of Edinburgh) within the Crystals program [Twin Law: 1 0 0 0 1 0 1 0 -1]. Application of the twin afforded improved residuals [R_1 ($I > 2\sigma(I)$) = 4.91%] with four molecules in the asymmetric unit.

2 A. Alberola, E. Carter, C.P. Constantinides, D.J. Eisler, D.M. Murphy and J.M. Rawson, *Chem. Commun.*, 2011, **47**, 2532.

Structure of **4**

In the case of **4** a monoclinic setting ($P2_1/c$) was initially determined [$a = 7.2196(4)$, $b = 11.8203(6)$, $c = 20.893(1)$, $\beta = 97.366(2)^\circ$] with two molecules (one dimer) in the asymmetric unit. Once again the data were moderately twinned and satisfactory refinement to acceptable residuals only proceeded smoothly once an appropriate twin law had been determined through the application of TwinRotMat within PLATON and an HKLF5 file generated for further refinement. The R values, K value, esds and background noise were all significantly improved, indicating the correct twin assignment to yield final $R_1 [I > 2\sigma(I) = 4.76\%]$. Notably a test for higher symmetry using ADDSYM detected a potential lattice centering or halving. When the suggested alternate cell ($a = 3.6099(8)$, $b = 11.8203(6)$, $c = 20.893(1)$, $\beta = 97.366^\circ$) was used, the structure solution obtained in this cell led to complete disorder of the dimeric molecule ($2 \times 50\%$ occupancy molecules), and so the larger cell was retained.

Structure of **5**

Compound **5** proved to be the most problematic of the series. An initial monoclinic C-centred cell was determined with a short crystallographic b -axis ($3.6366(1) \text{ \AA}$), three molecules in the asymmetric unit and an apparent regular π -stacked motif. However all three molecules revealed large anisotropic displacement parameters indicating similar problems to compounds **1** – **4**. Multiple crystals were studied in the range 100 – 273 K in order to try and clearly identify an appropriate super-cell but gave no clear indication of the larger cell dimensions. A series of other cells were examined in which the short axis was doubled and/or the angles relaxed to offer a lower symmetry triclinic structure. Most cells considered failed to provide satisfactory solutions but a low symmetry triclinic space group was identified which provided a π -stacked motif with 6 dimers in the asymmetric unit. Given the same trends in U_{ij} for the S and N atoms in the $C2/c$ setting of **5**, as had been observed for **1** – **4** we are confident that the true cell comprises a doubling of the short axis. Whilst the current triclinic setting provides substantially poorer residuals than the monoclinic setting both settings clearly reveal the same broad packing features. A comparison of the packing features in the two settings is presented in Figure S10. With a poor data:parameter ratio, only the S and Cl atoms were refined anisotropically in the lower symmetry triclinic setting.

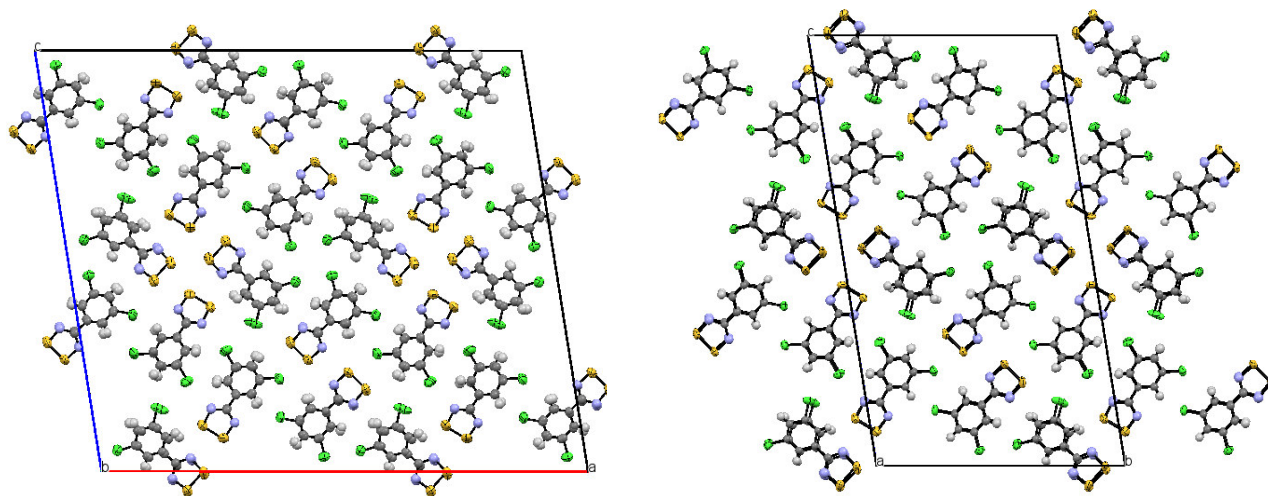


Figure S10 View of reduced monoclinic ($C2/c$) setting (left) and 'super-cell' ($P-1$) setting (right) of **5** viewed perpendicular to the stacking axis.

Weakening of the π^* - π^* dimerisation in 1,2,3,5-dithiadiazolyl radicalsC.P. Constantinides,^a D.J. Eisler,^a A. Alberola,^a E. Carter,^b D. Murphy^b and J.M. Rawson^{a,c*}

Table T3. Comparison of the ‘false’ high symmetry (grey background) and ‘true’ lower symmetry super-cell structures of **1 - 5**. The doubling of the crystallographic axes corresponding to the π -stacking direction are highlighted in red. N.B. Some discrepancies in unit cell parameters arise from different refinements when multiple data sets were measured.

Radical	Crystal System	Space Group	<i>a</i>	<i>B</i>	<i>C</i>	α	β	γ
1	Monoclinic	<i>P2₁/c</i>	3.6790(2)	13.6151(7)	17.9836(9)	90	101.781(3)	90
	Monoclinic	<i>P2₁/n</i>	7.3580(2)	13.615(3)	17.984(4)	90	101.78(3)	90
2	Monoclinic	<i>P2₁/c</i>	15.074(3)	3.621(1)	16.098(3)	90	91.16(3)	90
	Triclinic	<i>P-1</i>	15.057(3)	7.246(1)	15.986(3)	90	91.32(3)	90
3	Monoclinic	<i>P2₁/c</i>	3.6506(7)	24.358(5)	10.170(2)	90	97.54(3)	90
	Triclinic	<i>P-1</i>	7.3271(2)	10.3563(3)	24.6666(7)	88.096(2)	81.458(2)	77.009(1)
4	Monoclinic	<i>P2₁/c</i>	3.6099(8)	11.8203(6)	20.893(1)	90	97.366(2)	90
	Monoclinic	<i>P2₁/c</i>	7.2196(4)	11.8203(6)	20.893(1)	90	97.366(2)	90
5	Monoclinic	<i>C2/c</i>	41.5571(6)	3.6366(1)	36.426(2)	90	99.0583(7)	90
	Triclinic	<i>P-1</i>	7.2604(15)	20.872(4)	36.565(7)	98.49(3)	95.63(3)	95.10(3)

Weakening of the π^* - π^* dimerisation in 1,2,3,5-dithiadiazolyl radicals

C.P. Constantinides,^a D.J. Eisler,^a A. Alberola,^a E. Carter,^b D. Murphy^b and J.M. Rawson^{a,c}*